World Academy of Science, Engineering and Technology
International Journal of Chemical and Molecular Engineering
Vol:10, No:2, 2016

Influence of Organic Modifier Loading on Particle Dispersion of Biodegradable Polycaprolactone/ Montmorillonite Nanocomposites

O. I. H. Dimitry, N. A. Mansour, A. L. G. Saad

Abstract**—**Natural sodium montmorillonite (NaMMT), Cloisite Na^+ and two organophilic montmorillonites (OMMTs), Cloisites 20A and 15A were used. Polycaprolactone (PCL)/MMT composites containing 1, 3, 5, and 10 wt% of Cloisite Na^+ and PCL/OMMT nanocomposites containing 5 and 10 wt% of Cloisites 20A and 15A were prepared via solution intercalation technique to study the influence of organic modifier loading on particle dispersion of PCL/ NaMMT composites. Thermal stabilities of the obtained composites were characterized by thermal analysis using the thermogravimetric analyzer (TGA) which showed that in the presence of nitrogen flow the incorporation of 5 and 10 wt% of filler brings some decrease in PCL thermal stability in the sequence: Cloisite Na+>Cloisite 15A > Cloisite 20A, while in the presence of air flow these fillers scarcely influenced the thermoxidative stability of PCL by slightly accelerating the process. The interaction between PCL and silicate layers was studied by Fourier transform infrared (FTIR) spectroscopy which confirmed moderate interactions between nanometric silicate layers and PCL segments. The electrical conductivity (σ) which describes the ionic mobility of the systems was studied as a function of temperature and showed that σ of PCL was enhanced on increasing the modifier loading at filler content of 5 wt%, especially at higher temperatures in the sequence: Cloisite Na^+<Cloisite 20A<Cloisite 15A, and was then decreased to some extent with a further increase to 10 wt%. The activation energy E_σ obtained from the dependency of σ on temperature using Arrhenius equation was found to be lowest for the nanocomposite containing 5 wt% of Cloisite 15A. The dispersed behavior of clay in PCL matrix was evaluated by X-ray diffraction (XRD) and scanning electron microscopy (SEM) analyses which revealed partial intercalated structures in PCL/NaMMT composites and semi-intercalated/semi-exfoliated structures in PCL/OMMT nanocomposites containing 5 wt% of Cloisite 20A or Cloisite 15A.

Keywords**—**Polycaprolactone, organoclay, nanocomposite, montmorillonite, electrical conductivity, activation energy, exfoliation, intercalation.

I. Introduction

FILLING polymers with particles have been widely used as a method of improving the mechanical properties of the resulting composite materials, such as heat distortion temperatures, hardnesses, toughnesses, and mould shrinkages, as well as their fire resistances and electrical, and thermal conductivities; at high filler contents (sometimes>50 wt%) [1]. Such high filler levels increase the density of the product and can cause deterioration in these properties through interfacial incompatibility between the filler and the organic matrix [2].

Polymer nanocomposites represent a new class of polymeric materials [3], [4] that combine the properties of the nanoparticles (mechanical strength, modulus, and thermal stability) with processability and the flexibility of the organic polymer matrix [5]. These materials are particle filled polymers in which at least one dimension of the dispersed particles (i.e. length, width, or thickness) is in the nanometer range. Therefore, more interfacial interactions between the nanoparticles and the polymer matrix are expected. This will lead to improved thermal and mechanical properties for the related composite materials at much low filler contents, 3-5 wt% of the nanosized filler.

The most successful results have been obtained when using layered silicates (Fig. 1) [6] as nanofiller precursors, especially montmorillonite [7] (MMT), a mica-type silicate that consists of sheets arranged in a layered structure. It is widely used in a range of applications due to its high achievable surface area (about 750 m^2/g), platelet thickness of 1 nm, high cation exchange capacity, swelling capacity, and resulting strong adsorption/absorption capacities [8]. Due to the incompatibility between the hydrophilic layered silicates and hydrophobic polymer matrices, the individual platelets are not easily separated and dispersed in the organic polymer phase. Ion-exchange of the hydrophilic cations residing in the interlayer galleries space (e.g. Na^+) with various organic cations such as alkylammonium salt is needed in order to provide a partial hydrophobic character (organophilicity) to the originally hydrophilic silicate surfaces [9]. Intercalation of organic modifiers between silicate layers not only changes the surface properties from hydrophilic to hydrophobic, but also greatly increases the basal spacing of the layers [8]. These organic modifiers, therefore, lower the surface energy of silicate layers and enhance the miscibility between the silicate layers and the polymer matrix. By mechanically mixing it with the polymer matrix, the organically modified clay can be dispersed into small silicate stacks, or even into single platelets with a high aspect ratio (width to thickness). The resulting nanocomposites show large improvements in barrier properties [10], flame resistance [11], and dimensional stability, as well as in mechanical properties such as tensile strength, tensile modulus, and heat distortion temperature; without any significant loss of optical transparency, toughness, and impact strength [6], [12].

O. I. H. Dimitry and N. A. Mansour are with the Egyptian Petroleum Research Institute, Nasr City, Cairo,11727, Egypt (phone: +(202)22747847; fax: +(202)22747433; e-mail: research@epri.sci.eg).

A. L. G. Saad is with the National Research Centre, El Buhouth St. Dokki, Cairo,12311, Egypt (phone: +(202)33371362; fax: +(202)33370931).

Polymer nanocomposites have gained growing scientific and practical interest in the materials science community over the past decade due to their unique mechanical, optical, electrical, and magnetic properties; resulting from the homogeneous dispersion of ultrafine individual silicate platelets throughout the polymer matrix on a nanoscale. One of the main research and development domains, in which they are used, is the fabrication of nanocomposites for the electronics industry, where the rapid progress in computing technology always demands smaller components. Nano-technology utilizes objects with particle sizes from less than one up to hundreds of nanometers [13].

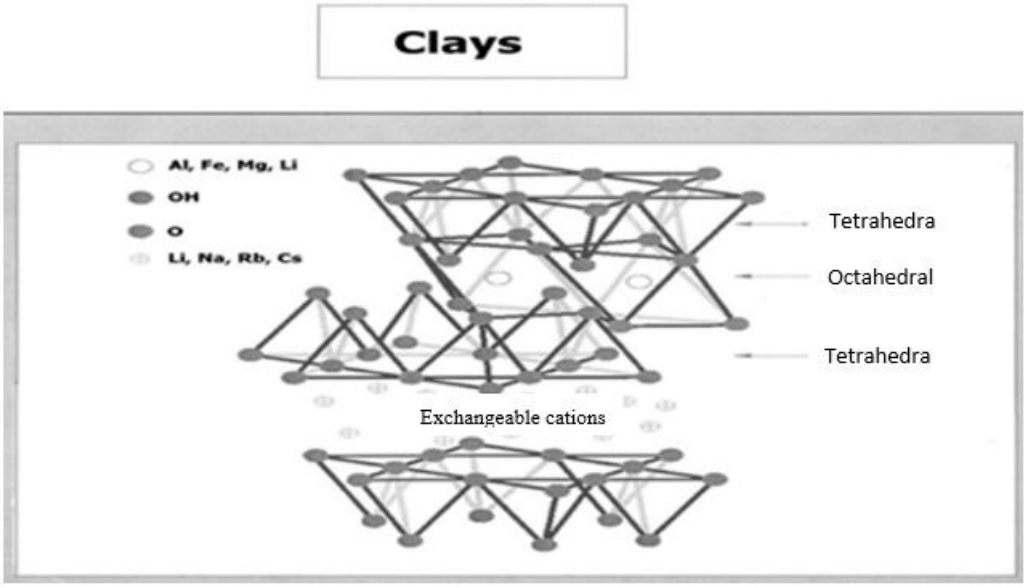

Fig. 1 The structure of a layered silicate [6]

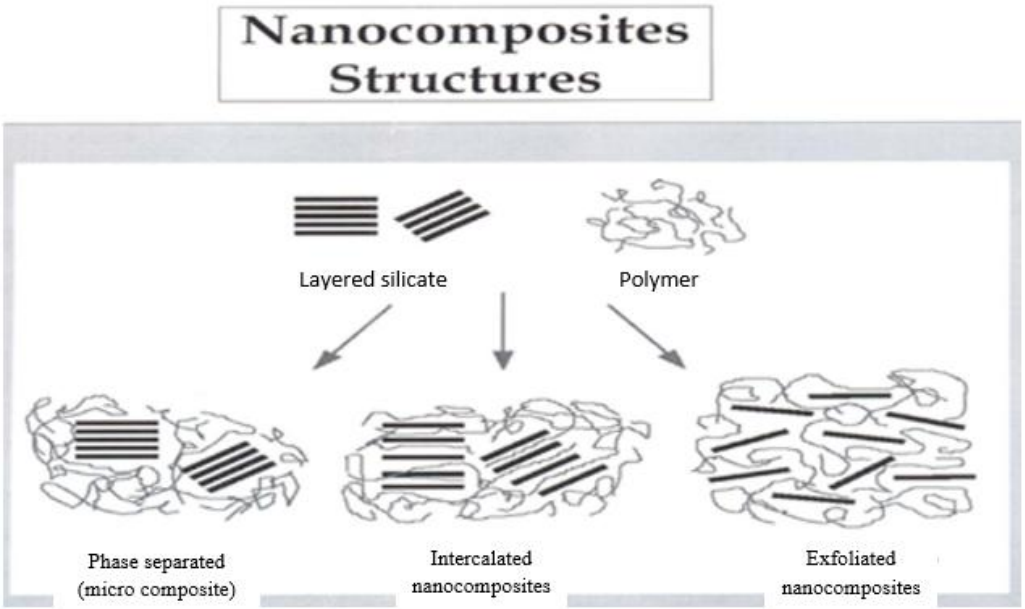

Fig. 2 Possible polymer-layered silicate structures [6]

The literature contains numerous studies concerning polymer nanocomposites based on various polymer matrices such as nylon 6 [14], epoxy resin [15], silicone rubber [16], polypropylene [17], polyethylene [18], poly(ethylene oxide) [19], PCL [20], polyimide [21], polyurethane [22], poly(vinyl chloride) [23], polystyrene [24], and poly(methyl methacrylate) [25].

Because the interaction between the polymer matrix and the nanoclay plays an important role in determining the phase-separation behavior and final morphology, it is important to determine whether the nanoclay intercalates or exfoliates in the polymer matrix (Fig. 2) [6]. The intercalated structure is a well-ordered multilayered structure of silicates, where the polymer chains are just inserted into the interlayer spaces. On

the other hand, the exfoliated/delaminated structure is more preferred for the maximum reinforcement of various properties, where the individual silicate layers in the nanometer range are uniformly dispersed in the polymer phase, and are no longer close enough to interact with one another [26]. Exfoliated nanocomposites usually provide the best property enhancement due to the large aspect ratio and surface area of the clay [27].

PCL is a semi-crystalline biodegradable, linear resorbable aliphatic polyester, whose repeat units are bonded via ester linkages, which are susceptible to hydrolysis when PCL is subjected to biodegradation. PCL is currently being studied for applications in agriculture, biomedical devices, pharmaceutical controlled release systems, and in biodegradable packaging purposes [28], [29]. The main drawback of PCL is its low melting point (65 ºC) which can be overcome by blending it with other polymers [30], [31] or by radiation cross-linking processes, resulting in enhanced properties for wide range of application [32]. The main limitations of PCL towards its wider industrial application are also its poor thermal and mechanical resistances and limited gas barrier properties [33]. These draw backs can be overcome by the addition of a small quantity of an environmentally benign material such as nano-sized fillers. Concerning all the potential nanocomposite precursors, those based on layered silicates have been the most extensively studied [34], [35] due to their availability and low cost. Several authors [36], [37] have recently reported the preparation and characterization of PCL-based nanocomposites with modified and unmodified MMTs; achieving greatly improved thermal, mechanical, and barrier properties compared with pristine PCL.

This article describes the preparation of three kinds of PCL-based composites and the thermal stability and FTIR spectroscopic investigations of the obtained products. The effects of adding 1, 3, 5, and 10 wt% of Cloisite Na^+ and 5 & 10 wt% of Cloisite 20A and Cloisite 15A on the electrical conductivity of PCL are also examined. A study of the activation energy E_σ of the PCL and its composites has been carried out. Furthermore, morphological studies of PCL composites have been conducted using XRD and SEM techniques.

II. Experimental

A. Materials

In this work, PCL (6-caprolactone polymer) obtained from Sigma-Aldrich Co. (product of Japan), having average Mw of 14.000 and average Mn of 10.000 by GPC was employed. MMT obtained from Southern Clay Products (Gonzales, TX, USA) was used as nanofiller. Its silicate layers are approximately 200 nm long and 1 nm thick, and the interlayer spacing between its stacked layers, denoted d_{001}, is about 1 nm [38]. Two different types of MMT were used: Cloisite Na^+, a natural MMT modified for higher Na content and two organophilic OMMTs, Cloisites 20A and 15A which are types of Cloisite Na^+ that has been modified with a quaternary ammonium salt. The organic modifier of Cloisites 20A and 15A is dimethyl dihydrogenated tallow ammonium cation, at a loading of 90 and 125 meq/100 g clay, respectively (Fig. 3), where tallow is ~ 65% $C_{18}H_{37}$; ~ 30% $C_{16}H_{33}$; ~ 5% $C_{14}H_{29}$. The long chain alkyl groups are used commonly in organoclays since they are within the range of favourable lengths for expanding the interlayer spacing and improving compatibility between the polymer matrix and the normally hydrophilic clay surface [39]. The alkyl groups of the organic modifier can also form van der Waals interactions with PCL soft segments [40].

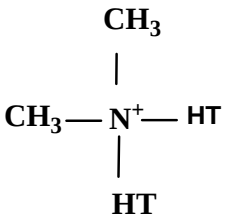

Fig. 3 Chemical modifier of Cloisites 20A and 15 A

Preparation of PCL/Clay Composites

PCL/composites were prepared by the solution intercalation technique. Initially, PCL was dissolved in chloroform (AR) at a concentration of 0.1 g/mL. A predetermined amount of well-dried Cloisitie Na+, Cloisite 20A, or Cloisite 15A was dispersed in 50 mL of chloroform and stirred by a magnetic stirrer for 1.5 h. The clay suspension was then sonicated for 0.5 h using a Branson Sonic Power s125 sonicator. This dispersion was added portionwise to the PCL solution and stirred vigorously at 60 °C for 1 h. The resulting PCL/clay solution was poured into a Petri dish and the PCL/clay composite was obtained after complete removal of chloroform. The thicknesses of the resulting PCL composite films ranged from 0.2 to 0.3 cm. The clay content of the produced film was 1, 3, 5, and 10 wt% of Cloisite Na^+ &5 and 10 wt% of Cloisite 20A or Cloisite 15A with respect to PCL.

B. Methods of Testing

1. TGA

The thermal stability of the prepared composites was studied using a TGA. All TGA spectra were recorded under a nitrogen and air atmosphere up to 500 °C using a programmed rate of 10 °C/min.

2. FTIR Spectroscopy

FTIR spectra were conducted by a Perkin-Elmer 1650 FTIR spectrophotometer using the KBr disk technique and the solvent used is toluene or chloroform. The FTIR spectrum was recorded at wave length of 500 to 4000 cm^{-1} and transmittance % from 40 to 100.

3. Electrical Conductivity

The electrical conductivity (σ) was calculated using:

$$\sigma = L/Rdc\ A \quad (1)$$

where L is the thickness of the sample in cm and A is its surface area in cm^2, while Rdc is the resistance in ohm.

The samples took the form of discs, 5 cm in diameter and 3 mm thick. The measurements were carried out at temperatures ranging from 25 to 55 °C using an ultrathermostat.

4. XRD Measurements

XRD patterns were obtained using a Siemens (Berlin, Germany) D500 diffractometer with a back monochromator and a Cu anticathode (step: 0.02°; step time: 1 s, temp.: 25 °C). Special attention was paid to the low 2θ region for accurate determination of d_{001} (i.e. the organoclay d-spacing).

5. SEM Testing

Phase morphology was studied using a JSM-5300 (JEOL, Tokyo, Japan) SEM. For scanning electron observations, the surface of the polymer was mounted on a standard specimen stub. A thin coating (~ 10^{-6} m) of gold was deposited into the polymer surface and attached to the stub prior to SEM examination in the microscope to avoid electrostatic charging during examination.

III. Results and Discussion

A. TGA

The thermal stabilities of the prepared composites were studied using TGA, where the weight loss due to the formation of volatile products after degradation at high temperature is monitored in function of a temperature ramp. PCL composites are characterized by a single weight loss with the beginning of the degradation shifted to much higher temperature. When the heating is operated under an inert gas flow (nitrogen, helium, ...), a non-oxidative degradation occurs while the use of air or oxygen allows to follow the oxidative degradation of the sample. The thermal degradation of PCL in inert atmosphere takes place through the rupture of the polyester chains via ester pyrolysis reaction with the release of CO_2, H_2O, and a carboxylic acid. In the case of polyester chains such as PCL, pyrolysis provokes chain cleavages randomly distributed along the chain and when two pyrolysis reactions occur with neighboring ester functions, one of the reaction products is 5-hexenoic acid [41]-[43].

The thermogravimetric behavior could be used as a proof of the interactions between the organic medium and the inorganic nanoplatelet surfaces. The results of TGA of the pristine PCL and PCL composites in the presence of nitrogen flow are shown in Figs. 4-6. The thermal stabilities of PCL and its composites from the TGA thermograms in nitrogen flow show that the temperature at which the PCL decomposition rate is highest is 410.83 °C. Fig. 4 shows that the introduction of 1 wt% and 3 wt% of Cloisite Na^+ into PCL slightly improves its thermal stability from 410.83 °C to 415.86 °C and 413.78 °C, respectively. At higher filler contents (5 wt% and 10 wt%), the thermal stabilization slightly decreases to 408.03 °C and 404.48 °C, probably as a result of the increased catalyzing effect of the clay itself toward the degradation of the PCL matrix [18]. Indeed, the incorporation of 5 wt% of Cloisite 15A and Cloisite 20A as shown in Figs. 5, 6 brings some decrease in PCL thermal stability from 410.83 °C to 394.11 °C and 385.23 °C, respectively and reaches 368.30 °C and 370.04 °C on further increasing the filler content to 10 wt%. This decrease in the thermal stability may be due to the moderate dispersion of Cloisite 15A or Cloisite 20A in PCL matrix which results from the moderate PCL/organoclay interactions according to FTIR and XRD results.

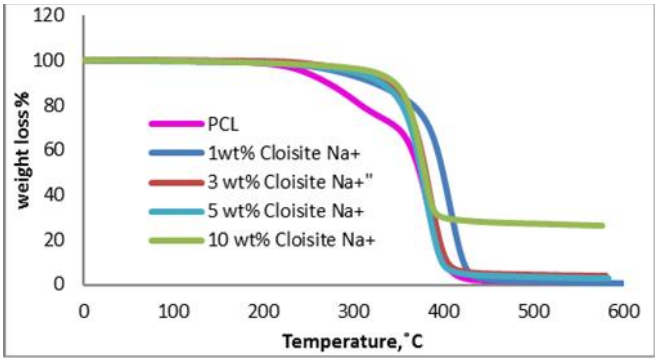

Fig. 4 TGA thermograms of PCL and PCL/1,3,5, 10 wt% Cloisite Na^+ composites in nitrogen atmosphere

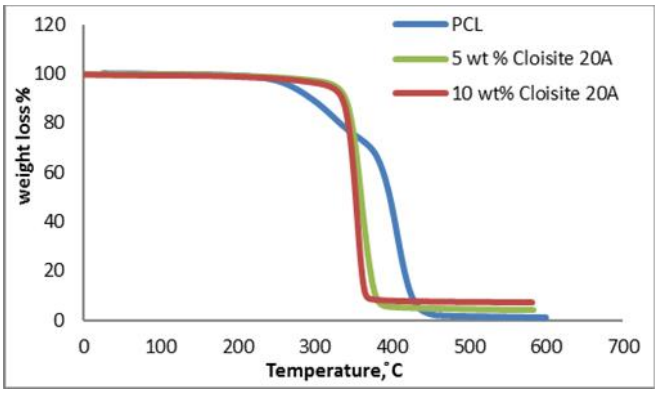

Fig. 5 TGA thermograms of PCL and PCL/5,10 wt% Cloisite 20A nanocomposites in nitrogen atmosphere

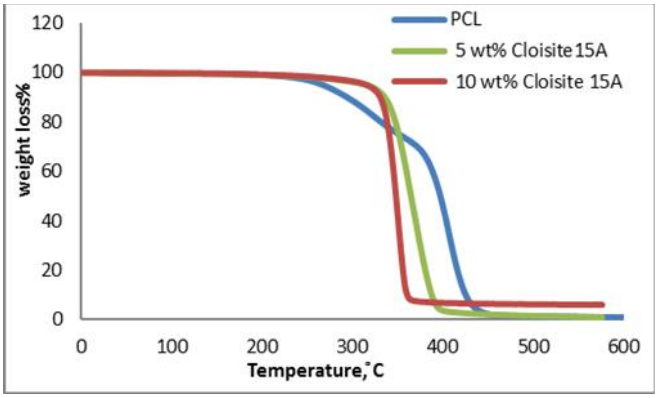

Fig. 6 TGA thermograms of PCL and PCL/5,10 wt% Cloisite 15A nanocomposites in nitrogen atmosphere

It has been reported in [44] that the introduction of very small amounts (1 wt%) of organophilic inorganic material improves the thermal stability of PCL matrix in the presence

of nitrogen, delaying the polymer weight loss; while an increase in the organoclay loading destabilizes the polymer matrix by decreasing the temperature of the decomposition initiation. This may be attributed to the rise of the organic modifier's content, which exhibits a reduced onset decomposition temperature compared with the pristine polymer [45]. Apparently, the layered silicates catalyze PCL pyrolysis due to the catalytic action of the clays, resulted from the presence of Lewis acidic sites [46] which are created upon organic modifier degradation. As a result, the thermal resistances of PCL/organoclay nanocomposites are lower than that of pristine PCL, especially those having higher organoclay loading i.e., higher organic modifiers content.

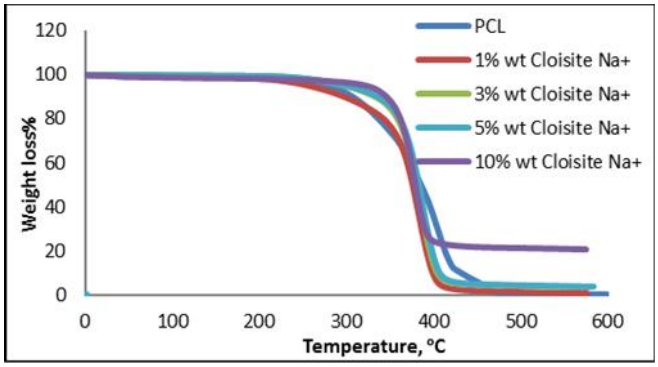

Fig. 7 TGA thermograms of PCL and PCL/1,3,5,10 wt% Cloisite Na^+ composites in air atmosphere

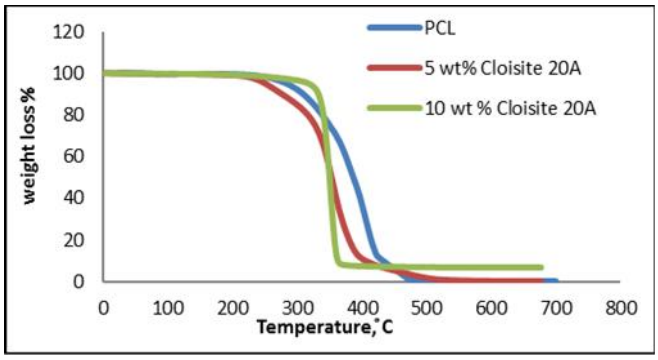

Fig. 8 TGA thermograms of PCL and PCL/5,10 wt% Cloisite 20A nanocomposites in air atmosphere

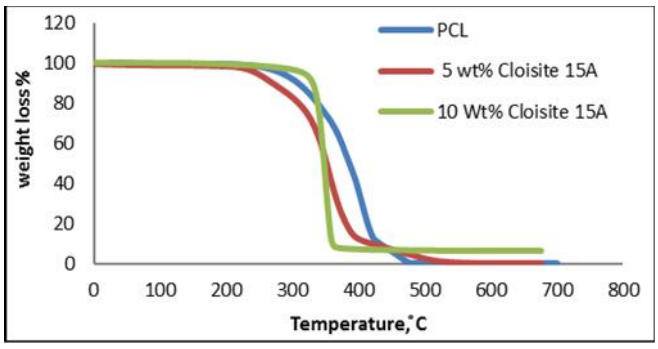

Fig. 9 TGA thermograms of PCL and PCL/5,10 wt% Cloisite 15A nanocomposites in air atmosphere

Thermal degradation studies were also performed in the presence of air flow. Even though it has been reported [47], [48] that the presence of well-dispersed inorganic platelets usually delays the diffusion of oxygen from the air to the polymer mass and retards the escape of the volatile products produced during decomposition, thereby improving the polymer stability, in the present case, the introduction of the silicate sheets leads to an increase in the rate of PCL mass volatilization and hence, to a decrease in PCL thermal stabilization, as illustrated in Figs. 7-9. For instance, Fig. 7 shows that for Cloisite Na^+, the thermal stability of PCL increases from 429.55 °C to 436.91 °C and 433.49 °C at filler contents of 1 wt% and 3 wt%, respectively and then decreases to 425.54 °C and 420.32 °C at higher filler contents (5 wt% and 10 wt%). Figs. 8, 9 also show that for Cloisite 15A and Cloisite 20A, PCL thermal stability decreases from 429.55 °C to 409.36 °C and 402.48 °C, respectively at organoclay loading of 5wt% and then decreases to 370.90 °C and 366.96 °C at 10 wt% loading. It is apparent from these results that the thermal stabilities of PCL and its composites are higher in the presence of air than those in the presence of nitrogen. This means that thermal degradation to volatile products takes place at a lower temperature in the presence of oxygen than that in the presence of nitrogen. These results indicate that Cloisite 15A and Cloisite 20A scarcely influence the thermoxidative stability of PCL by slightly accelerating the process [49].

In conclusion, in the presence of nitrogen and air, the incorporation of filler brings some decrease in PCL thermal stability in the sequence: Cloisite Na^+> Cloisite 15A> Cloisite 20A, and with higher values of thermal stability in presence of air.

B. FTIR Spectroscopy

Figs. 10, 13, or 15 and 14 or 16 show the FTIR spectra of pristine PCL, Cloisite 20A or Cloisite 15A and PCL/5 wt% of Cloisite 20A or Cloisite 15A nanocomposite, respectively. As seen in Figs. 13 or 15, five new absorption peaks are found at 2923.33 or 2923.36 cm^{-1}, 2851.80 or 2852.24 cm^{-1}, 1471.44 or 1471.35 cm^{-1}, 725.51 or 723.62 cm^{-1}, and 1376.53 or 1372.66 cm^{-1} in the FTIR spectrum of Cloisite 20A or Cloisite 15A. The absorptions at 2923.33 or 2923.36 cm^{-1} and 2851.80 or 2852.24 cm^{-1} can be attributed to asymmetric and symmetric stretching vibrations of C-H bands, whereas the absorption at 1471.44 or 1471.35 cm^{-1} and 725.51 or 723.62 cm^{-1} can be attributed to the CH_2 methylene bending and rocking vibrations, and the absorption at 1376.53 or 1372.66 cm^{-1} can be attributed to CH_3 vibration [18], [50], [51]; indicating that the organic modifier of Cloisite 20A or Cloisite 15A has been exchanged into the galleries of the silicate layers of Cloisite Na^+ (NaMMT), Fig. 11.

Figs. 12, 14, or 16 show that PCL/5 wt% of Cloisite Na^+ composite, PCL/5 wt% of Cloisite 20A, or Cloisite 15A nanocomposite have similar bands to those characteristic of MMT: 1046.95, 1045.44, or 1044.90 cm^{-1}; 520.50, 521.02, or 520.57 cm^{-1}; and 458.57, 458.22, or 457.31 cm^{-1}, corresponding to the stretching vibration of Si-O-Si, the

stretching vibration of Al-O, and the bending vibration of Si-O, respectively [52], [53]. These bands indicate that the PCL chains have intercalated into the gallery of layered silicates [54]. It has also been found that the positions of peaks from distinctive functional groups are nearly identical in both pristine PCL (Fig. 10) and PCL/Cloisite 20A or Cloisite 15A nanocomposite (Figs. 14 or 16), which means that the segmented structure of PCL is not affected by the presence of organoclay [55].

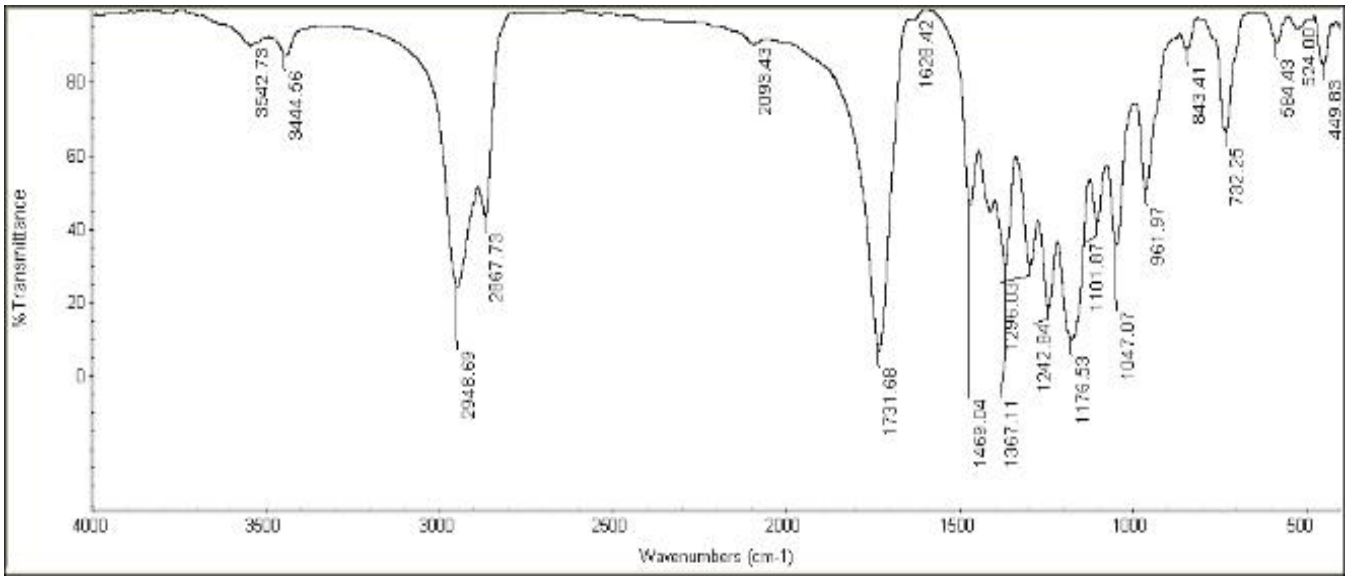

Fig. 10 FTIR spectrum of PCL

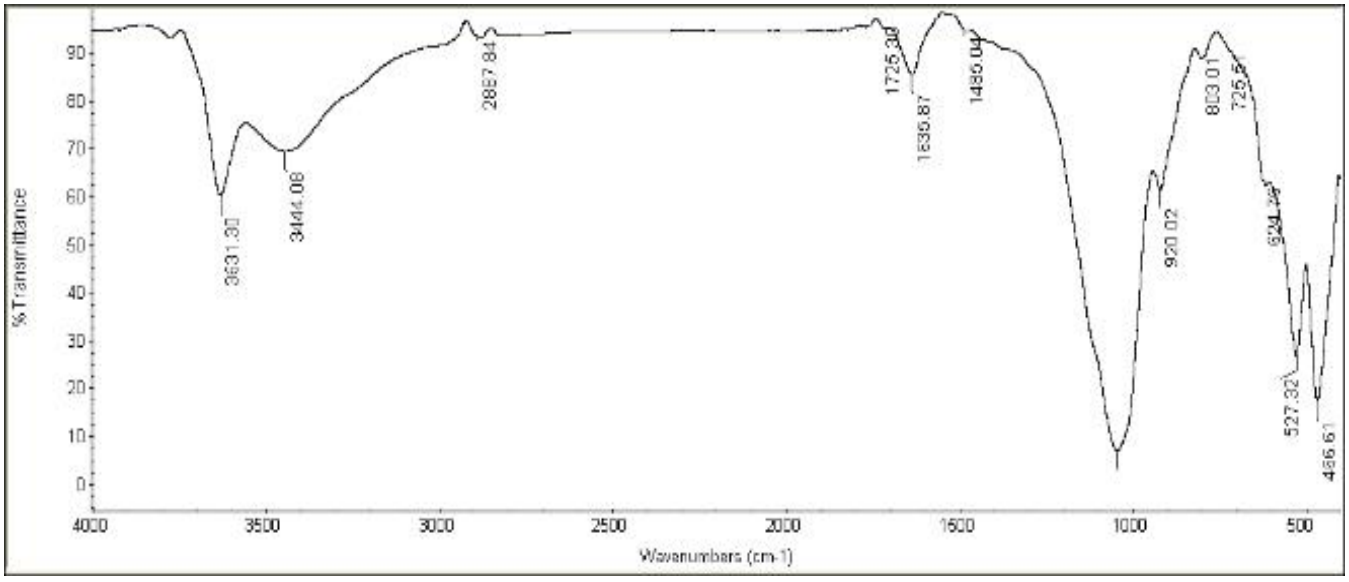

Fig. 11 FTIR spectrum of Cloisite Na^+

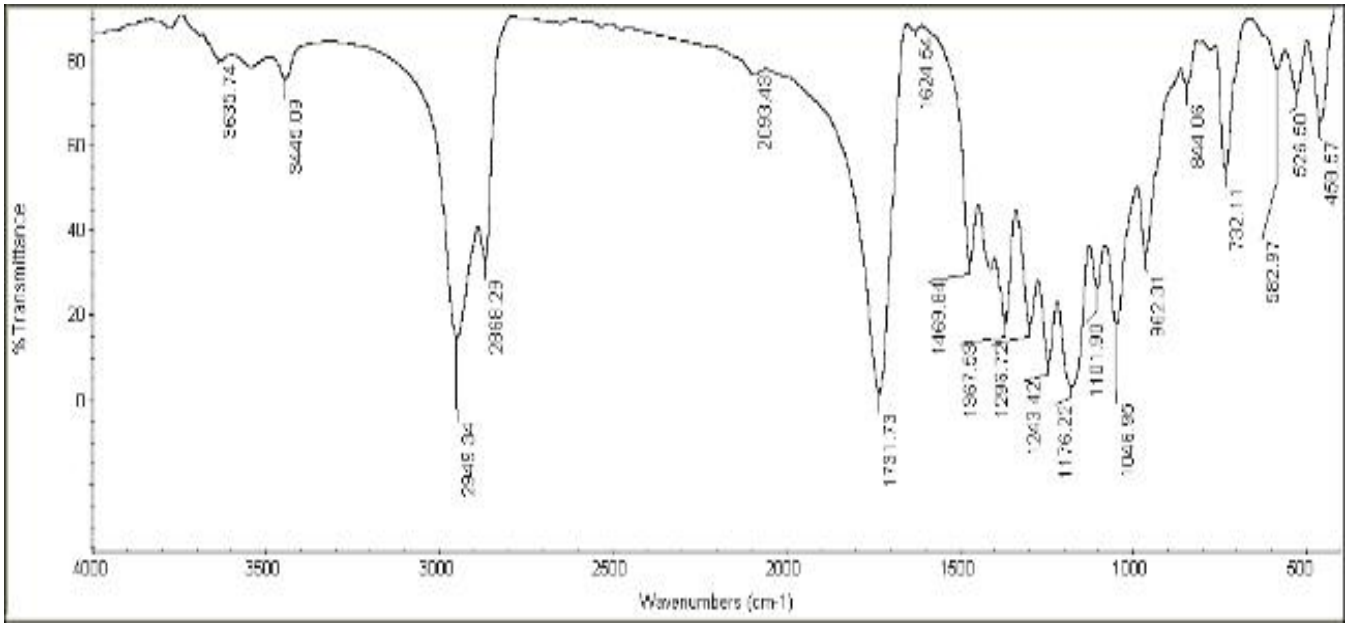

Fig. 12 FTIR spectrum of PCL/5 wt% Cloisite Na+ composite

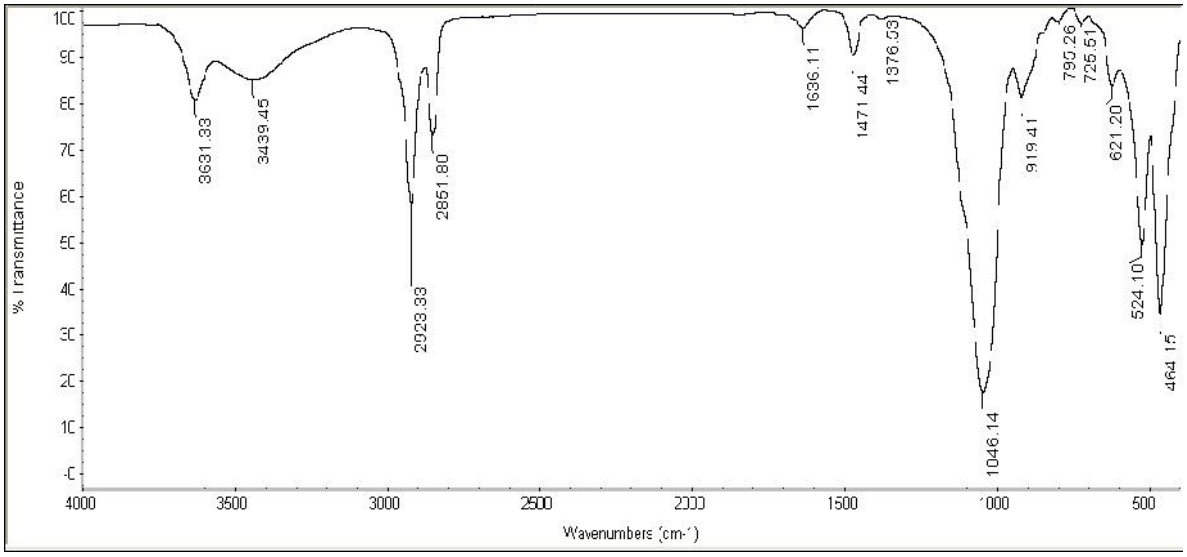

Fig. 13 FTIR spectrum of Cloisite 20A

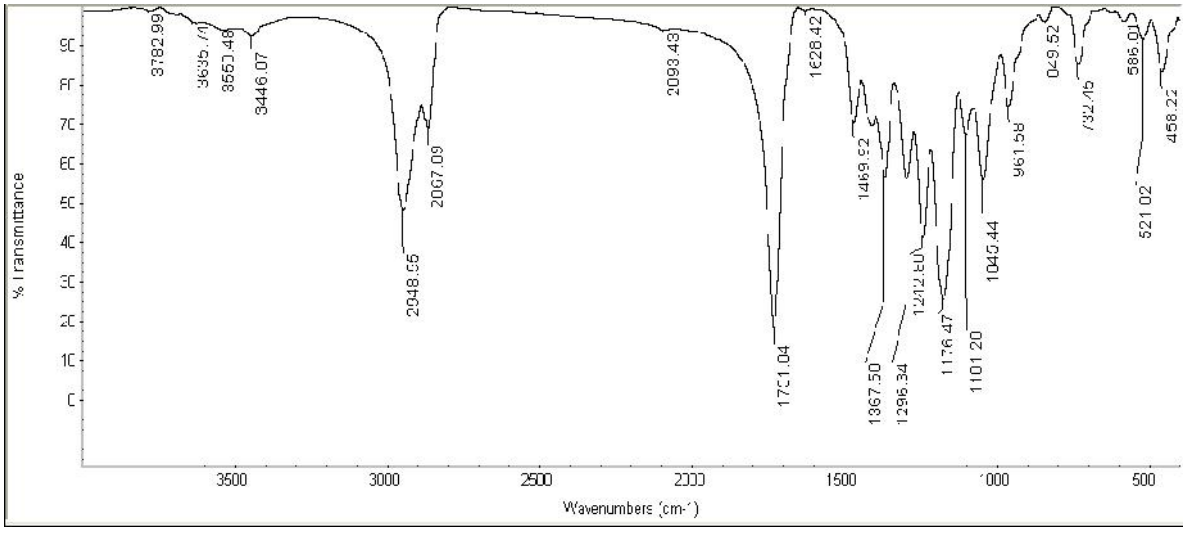

Fig. 14 FTIR spectrum of PCL/5 wt% Cloisite 20A nanocomposite

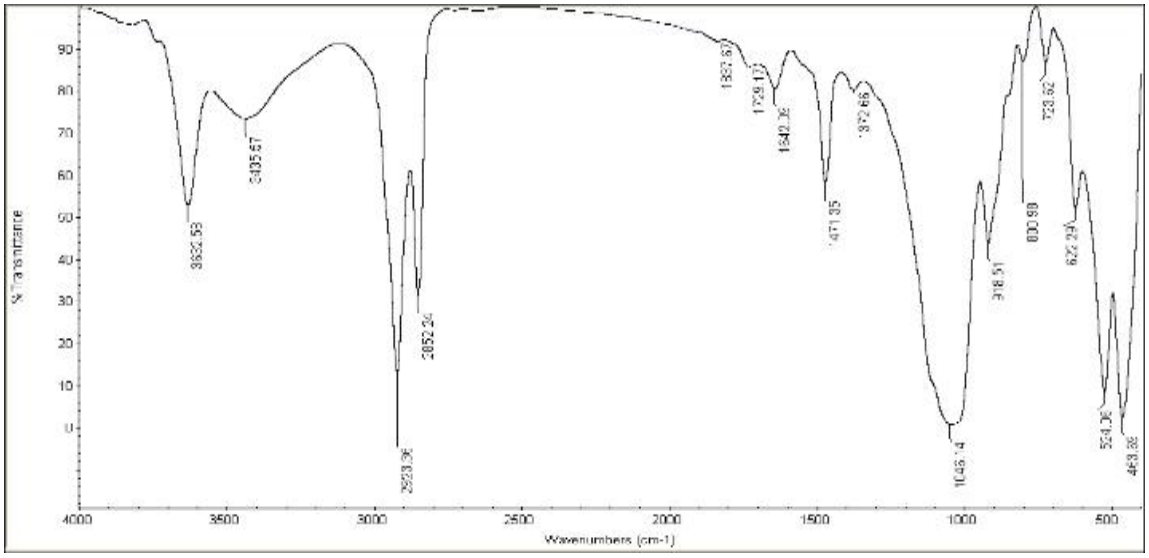

Fig. 15 FTIR spectrum of Cloisite 15A

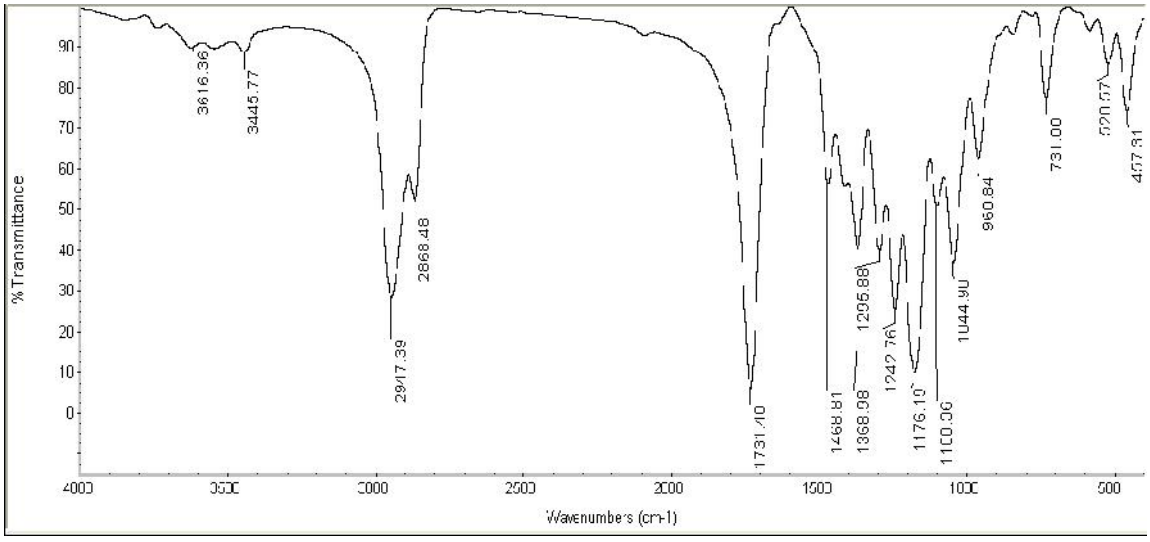

Fig. 16 FTIR spectrum of PCL/5 wt% Cloisite 15A nanocomposite

The FTIR spectrum of PCL/Cloisite Na^+ composite, PCL/ Cloisite 20A, or Cloisite15A nanocomposite (Figs. 12, 14, or 16) also shows a distinct absorption at 1731.13, 1731.84, or 1731.40 cm^{-1}, corresponding to the stretching vibration of free C=O; and 1176.22, 1176.47, or 1176.19 cm^{-1}, corresponding to the stretching vibration of C-O; which are the characteristic bands of PCL (Fig. 10) [56]. These results show that PCL chains are immobilized inside and/or on the layered silicates, which may confirm the interaction between the silicate layers and PCL. Moreover, the presence of the free C=O band located at 1731.84 or 1731.40 cm^{-1} and the absence of the hydrogen-bonded C=O band from the OCL groups which is usually appeared at approximately 1701 cm^{-1} in the FTIR spectrum of PCL/Cloisite 20A or Cloisite 15A nanocomposite in Figs. 14 or 16, indicate that there is no hydrogen bonding between the organic modifier of Cloisite 20A or Cloisite 15A and the PCL. This implies that PCL can be absorbed on the silicate surface by the van der Waals interaction forces between the nonpolar alkyl chains of the organically modified clay and the soft segments of the PCL [40], [57]. In addition, more favorable interaction between the ester group of OCL:

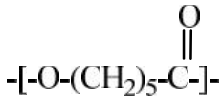

and the positively charged ammonium headgroup of organic modifier may be established due to their polar nature. On the other hand, Figs. 11, 13, or 15 show two peaks at 3631.30, 3631.33, or 3632.58 cm^{-1} and 1635.87, 1636.11, or 1642.09 cm^{-1}, corresponding to the stretching vibration and bending vibration of the -OH groups in the clay sample [40]. The absorption in these bands is relatively small compared to those due to -CH stretching. The FTIR spectra of the composites (Figs. 12, 14, and 16) show that most of these structural -OH groups that exist on the surface of the silicate layers are disappeared which may indicate that they could have participated in the clay-PCL tethering reactions [58], [59].

C. Electrical Properties

1. Electrical Conductivity

One of the interesting features of electrical conductivity (σ) is its temperature dependence, which allows us to understand conduction mechanisms in materials. Figs. 17 and 18 show the temperature dependences of the electrical conductivities of PCL and the composites containing Cloisite Na^+, Cloisite 20A, and Cloisite 15A. It is evident from these figures that σ of PCL and these composites increases with increasing temperature from 25 to 55 °C due to the increased mobilities of ionic bodies that occur as a result of excitation by heating. This characterizes semiconductor-like conduction in these composites. Furthermore, Fig. 17, which shows the relation between σ and NaMMT content at temperatures from 25 to 55℃ and quantitatively summarizes the data presented in Table I, shows an increase in the values of σ of PCL with increasing NaMMT content up to 5 wt%, especially in the lower frequency region and at higher temperatures and some decrease with a further increase to 10 wt%. Fig. 18, which quantitatively summarizes the data presented in Table II, also shows considerable increase in the values of σ of PCL with increasing the organic modifier loading at filler content of 5 wt% in the sequence: Cloisite Na^+ < Cloisite 20A < Cloisite 15A. The obtained values are situated between the two extremities of those of semiconductors (10^{-10} – 10^{+2} Ω^{-1} cm^{-1}) [60]. At 10 wt% content of the filler, the values of σ decrease to some extent. This may be attributed to the formation of some nanoparticle agglomerates due to more intense interfacial interactions between nanoparticles rather than between nanoparticle and PCL matrix upon further increasing the content of the filler, which may cause some steric hindrance that partially contributes to decreasing the electrical charge mobility, and hence to decreasing the electrical conductivity.

Different conduction mechanisms are possible in polymers [61], [62]. Almost all of the mechanisms are related to different types of polarization that can occur in the system. Each of these mechanisms predominates for a given temperature range and applied electric field.

TABLE I
ELECTRICAL CONDUCTIVITY (σ) OF PCL MIXED WITH VARIOUS PROPORTIONS OF CLOISITE NA

Temp.(t,˚C)/Sample	σx10 ^{10} (Ω^{-1} cm^{-1}) at various proportions of Cloisite Na^+				
	PCL	PCL-1wt% Cloisite Na^+	PCL-3 wt% Cloisite Na^+	PCL-5 wt% Cloisite Na^+	PCL-10 wt% Cloisite Na^+
25	0.35	0.62	1.01	1.37	0.9
30	0.46	0.8	1.27	1.63	1.16
35	0.57	1.06	1.56	2.01	1.39
40	0.74	1.27	1.92	2.55	1.76
45	0.93	1.68	2.49	2.99	2.27
50	1.17	2.02	2.99	3.51	2.73
55	1.49	2.49	3.68	4.13	3.27

TABLE II
ELECTRICAL CONDUCTIVITY (Σ) OF PCL MIXED WITH 5 AND 10 WT% OF CLOISITE NA+, CLOISITE 20A, AND CLOISITE 15A

Temp.(t,°C)/ Sample	σx10^{10} (Ω^{-1} cm^{-1}) at 5 and 10 wt% of Cloisites Na$^+$,20A, and 15A						
	PCL	PCL-5 wt% Cloisite Na$^+$	PCL-5 wt% Cloisite 20 A	PCL-5 wt% Cloisite 15 A	PCL-10 wt% Cloisite Na$^+$	PCL-10 wt% Cloisite 20 A	PCL-10 wt% Cloisite 15 A
25	0.35	1.37	3.27	5.84	0.9	2.49	4.21
30	0.46	1.63	3.85	6.85	1.16	2.86	5.07
35	0.57	2.01	4.51	7.86	1.39	3.43	5.96
40	0.74	2.55	5.44	8.82	1.76	4.12	6.83
45	0.93	2.99	6.53	10.6	2.27	5.19	8.05
50	1.17	3.51	7.86	12.16	2.73	5.96	9.45
55	1.49	4.13	9.02	14.6	3.27	6.83	11.1

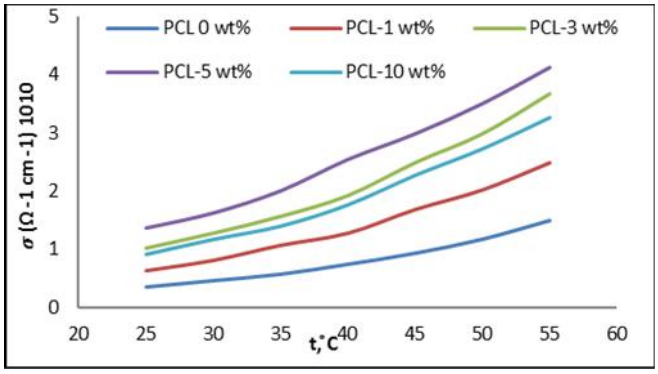

Fig. 17 Dependence of the electrical conductivity (σ) on the temperature (t) for PCL mixed with various proportions of Cloisite Na+ (0,1,3,5,and 10 wt%)

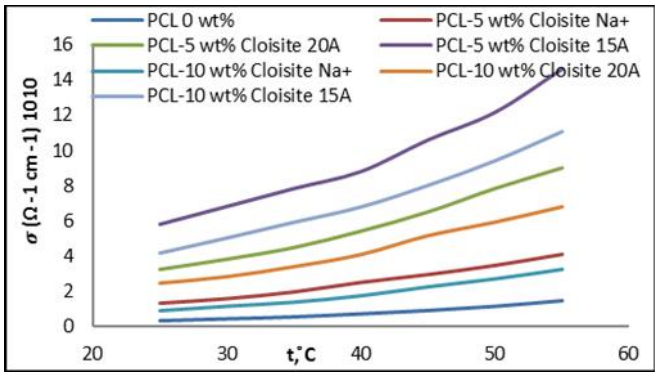

Fig. 18 Dependence of the electrical conductivity (σ) on the temperature (t) for PCL mixed with 5 and 10 wt% of Cloisite Na+, Cloisite 20A, and Cloisite 15A

2. Activation Energy (E_σ)

The temperature dependence of the electrical conductivity (σ) can be expressed by the Arrhenius equation:

$$\sigma = \sigma_o \exp(-E_\sigma/kT) \quad (2)$$

where E_σ is the activation energy for σ, k is the Boltzmann constant, T is the absolute temperature, and σ_o is a pre-exponential factor depending on the mobilities of the charge carriers. The corresponding parts of logσ versus 1/T plots were interpolated by straight lines, as shown in Figs. 19, 20. These results indicate that the PCL composites of 1,3,5, and 10 wt% of Cloisite Na$^+$ and PCL nanocomposites of 5 and 10 wt% of Cloisite 20A and Cloisite 15A tend to behave as semiconductors. From the slope of the straight line, the activation energies E_σ were estimated and are given in Tables III and IV.

TABLE III
ACTIVATION ENERGY (E_ε) OF PCL MIXED WITH VARIOUS PROPORTIONS OF CLOISITE NA$^+$

Samples[a]	Activation Energy (Kcal/mol)
PCL-0	4.24
PCL -1	3.97
PCL -3	3.68
PCL -5	3.48
PCL -10	3.73

[a] The numbers in the names of the samples indicate the content of Cloisite Na+; for example, PCL-5 means a sample with 5 wt% of Cloisite Na+.

TABLE IV
ACTIVATION ENERGY (E_ε) OF PCL MIXED WITH 5 AND 10 WT% OF CLOISITE NA$^+$, CLOISITE 15A, AND CLOISITE 20A

Samples	Activation Energy (Kcal/mol)
PCL	4.24
PCL-5 wt% Cloisite Na$^+$	3.48
PCL-5 wt% Cloisite 20A	2.85
PCL-5 wt% Cloisite 15A	2.35
PCL-10 wt% Cloisite Na$^+$	3.73
PCL-10 wt% Cloisite 20A	3.14
PCL-10 wt% Cloisite 15A	2.57

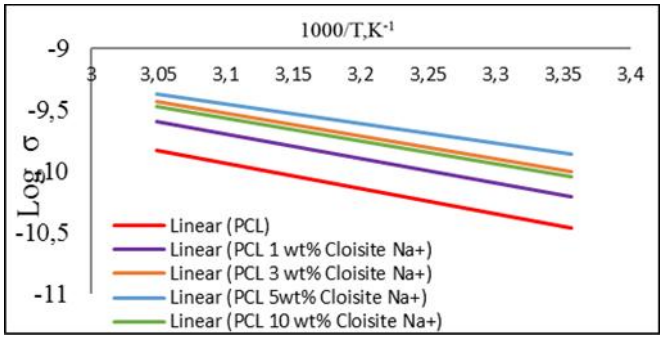

Fig. 19 Dependence of log σ on 10^3/T for PCL mixed with various proportions of Cloisite Na+ (0, 1,3,5, and 10 wt%)

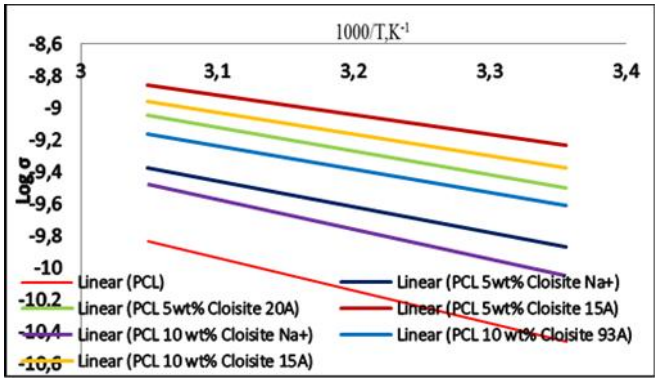

Fig. 20 Dependence of log σ on 10^3/T for PCL mixed with 5 and 10 wt% of Cloisite Na+, Cloisite 20A, and Cloisite 15A

It has been found that the period of excitation depends on the activation energy to make the substance conducting. If the activation energy is low i.e., the system is easily excited, the PCL composite becomes semiconducting at room temperature or in the presence of indirect light. Hence, it can be used for electronic devices working at ambient temperature. It is apparent from Table III that E_σ of PCL decreases with increasing the clay content up to 5 wt% and decreases to a lesser extent at 10 wt% content of the filler. Table IV also shows that the lowest value of E_σ for PCL/5 wt% Cloisite 15A nanocomposite (2.35 Kcal/mol) indicates that it is easily excited and tends to behave as a semiconductor, so it can be better employed for electronic and microwave nanodevices.

D. Morphologies of the PCL/Composites

The dispersed behavior of organoclay particles in PCL matrix has been identified by XRD and SEM analyses.

1. XRD Analysis

XRD is the most commonly used method to assess the morphology of the nanoclay in either powder form or when compounded into a polymer matrix. The X-rays are reflected from each clay layer within a sample, so there is a relationship between the angle θ and the physical spacing in the system. At small angles, the diffraction peak position is related to the interlayer spacing according to Bragg's law: $n\lambda = 2d \sin \theta$, where n is the order of interference, λ is the wavelength of the X-rays used, d is the spacing between the diffraction planes, and θ is the measured diffraction angle. One of the limitations of XRD analysis is that it may not always yield a unique interpretation of the data. Often, other techniques must be used to complement the diffraction experiments [63]. XRD characterization is generally based on a comparison between the diffraction peak position of the nanoclay powder and that of the nanoclay in the polymer matrix [17].

The XRD pattern of Cloisite Na^+ (NaMMT) shows a characteristic diffraction peak (d_{001} plane) at 2 θ = 7.54º, corresponding to basal spacing of 11.69 Å (Fig. 21). When NaMMT is modified by organic modifier, the gallery of MMT is intercalated and expanded by the molecular chain of the organic modifier. The XRD pattern of Cloisite 20A shows a characteristic diffraction peak (d_{001} plane) at 2θ=3.33º, corresponding to basal spacing of 26.50 Å (Fig. 22) while the XRD pattern of Cloisite 15A exhibits a characteristic diffraction peak (d_{001} plane) at 2θ=2.78º, corresponding to basal spacing of 31.75Å (Fig. 23).

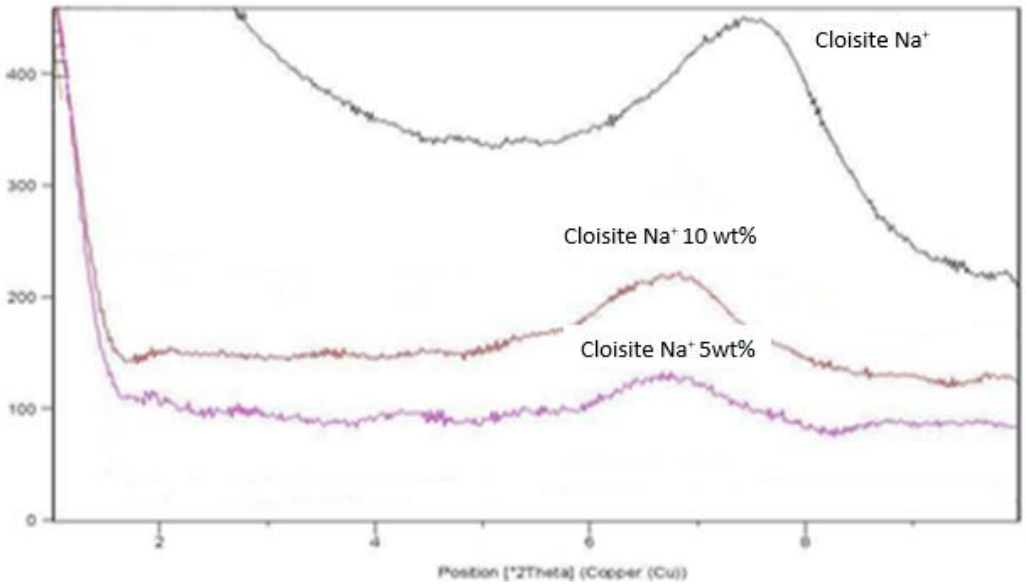

Fig. 21 XRD Patterns of Cloisite Na+ and PCL/5 and 10 wt% Cloisite Na+ composites

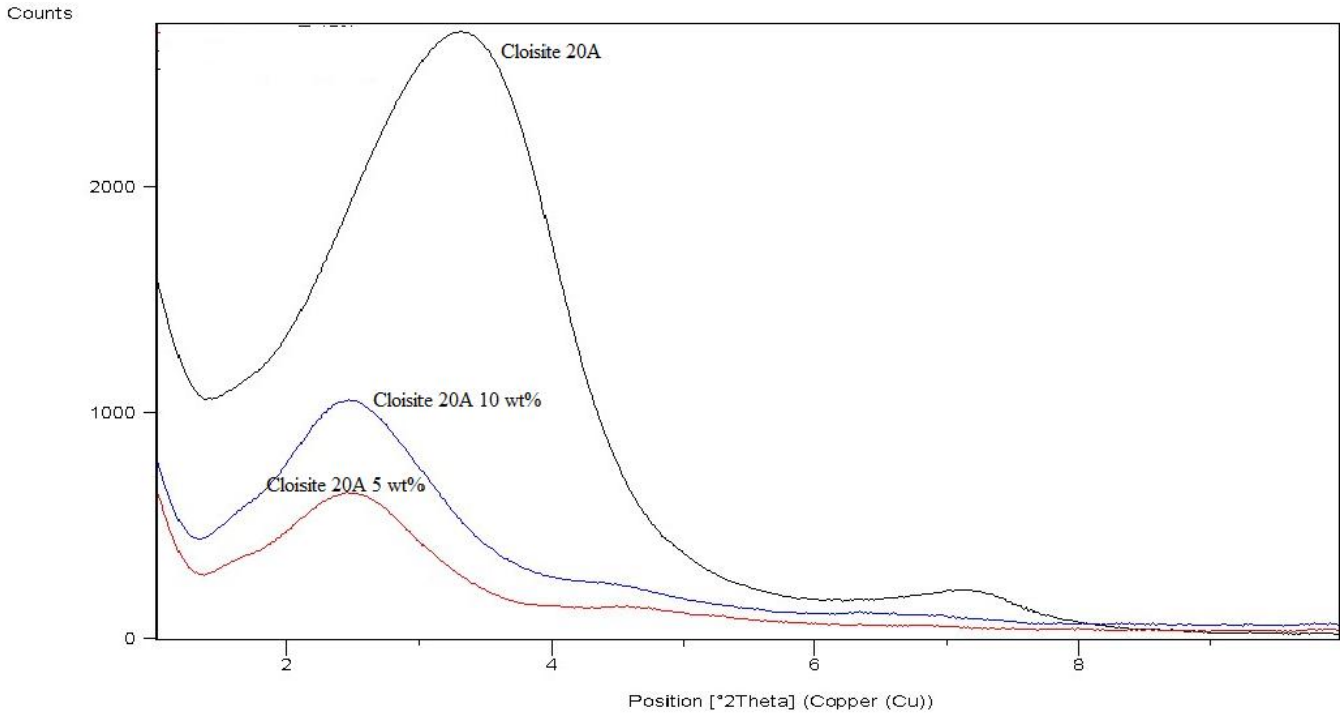

Fig. 22 XRD Patterns of Cloisite 20A and PCL/5 and10 wt% Cloisite 20A nanocomposites

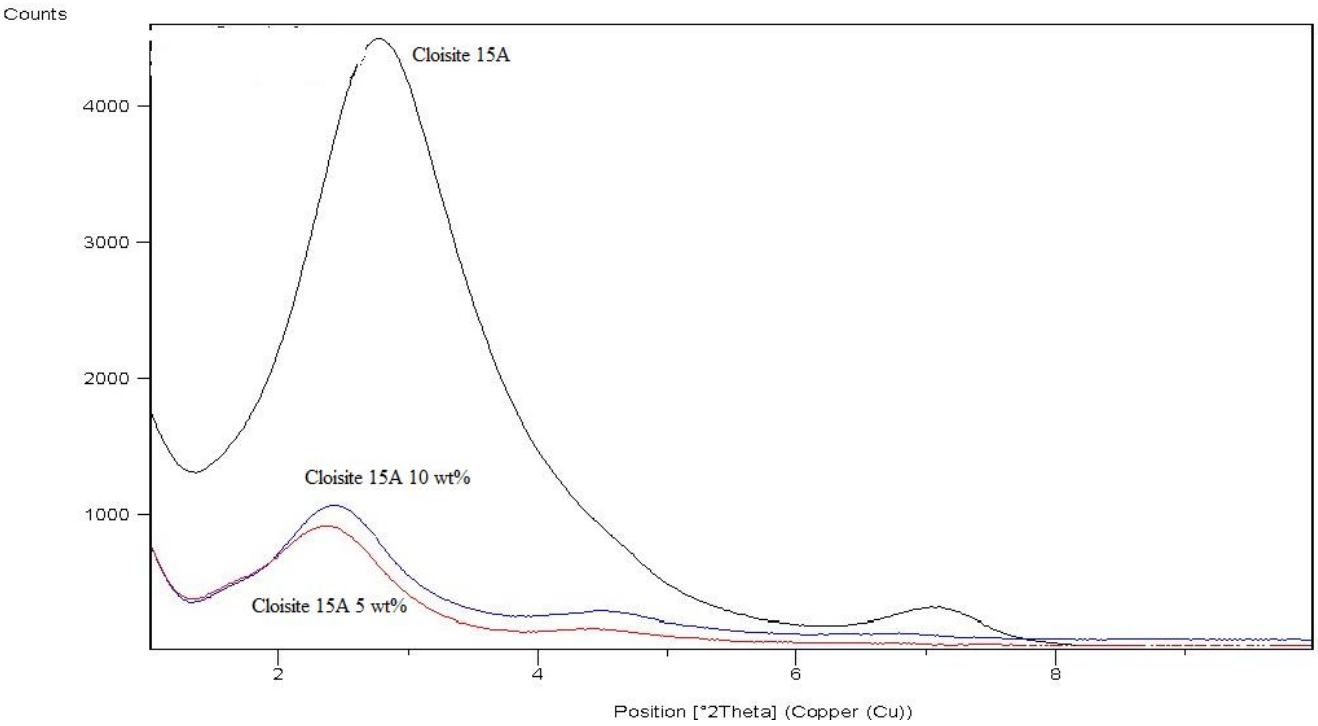

Fig. 23 XRD Patterns of Cloisite 15A and PCL/5 and 10 wt% Cloisite 15A nanocomposites

In compounded samples, the increased clay spacing due to the addition of PCL between the platelets is evident. The XRD patterns of Cloisite Na^+ and the PCL/NaMMT composites with 5 and 10 wt% of Cloisite Na^+ are shown in Fig. 21. For PCL/5 and 10 wt% of NaMMT composites, the shift of the diffraction peak from the (d_{001} plane) of Cloisite Na^+ from 2 θ = 7.54º to 2 θ = 6.60º and 6.77º shows a slight increase in the interlayer spacing from 11.69 Å to 13.39 Å and 13.04 Å, respectively indicating that microcomposites with micron-sized particles dispersed in PCL are formed rather than nanocomposites with few nano-sized particles dispersed in PCL; resulting in partially intercalated structures.

The gallery spacing of organoclay (OMMT) in polymer nanocomposites generally depends on the interaction between the polymer matrix and OMMT [64], [65]. The XRD patterns of Cloisite 20A and the PCL/OMMT nanocomposites with 5 and 10 wt% of Cloisite 20A are shown in Fig. 22 and those of Cloisite 15A and the PCL/OMMT nanocomposites of 5 and 10 wt% of Cloisite 15A are shown in Fig. 23. For PCL/5 and 10 wt% of Cloisite 20A nanocomposites, the shift of the diffraction peak from the (d_{oo1} plane) of Cloisite 20A from 2 θ = 3.33˚ to 2 θ = 2.47˚ and 2 θ = 2.48˚ shows an increase in the interlayer spacing from 26.50 Å to 35.73 Å and 35.64 Å, respectively. For PCL/5 and 10 wt% of Cloisite 15A nanocomposites, the shift of the diffraction peak from the (d_{oo1} plane) of Cloisite 15A from 2 θ = 2.78˚ to 2 θ = 2.36˚ and 2 θ = 2.43˚ shows an increase in the interlayer spacing from 31.75 Å to 37.32 Å and 36.31 Å, respectively. These results indicate that the PCL molecular chains have diffused into the galleries of silicate layers, expanding the clay structure to form a well-ordered multilayered structure consisting of layers of PCL molecular chains alternating with layers of layered silicate [9], [66]. This means that the morphology of these composites is mainly intercalated, even though exfoliated clay platelets may coexist; especially at 5 wt% of organoclay i.e., at low level of nanoparticle agglomeration. In this respect, a broad peak is observed at 2 θ = 2.47˚ and 2 θ = 2.36˚ for Cloisite 20A and Cloisite 15A, respectively which may indicate that both intercalation and exfoliation exist in the PCL matrix [67]. It is also apparent from these results that the diffraction peak from the (d_{oo1} plane) of Cloisite 15A is shifted to lower diffraction angle than that of Cloisite 20A, indicating that the nanocomposite of Cloisite 15A has a higher level of intercalation and exfoliation.

The shift of an XRD peak to a lower angle is not sufficient to identify a material as only intercalated. Frequently, mixtures of intercalated and exfoliated structures are obtained and this requires SEM for characterization [68].

2. SEM Characterization

The degree of nanometer-scale dispersion of silicate layers in PCL matrix has been confirmed by SEM micrographs. Fig. 24 shows SEM micrographs of PCL/5 and 10 wt% of Cloisite Na^+: PCL-5 (a) and PCL-10 (b), indicating partially intercalated structures which are in agreement with the presence of the peak in XRD. Fig. 25 shows SEM micrograph of PCL/5 and 10 wt% of Cloisite 20A: PCL-5 (a) and PCL-10 (b). Fig. 26 also shows SEM micrograph of PCL/5 and 10 wt% of Cloisite 15A: PCL-5 (a) and PCL-10 (b). Figs. 25 (a) and 26 (a) show SEM micrographs of PCL/5 wt% of Cloisites 20A and 15A nanocomposites, respectively and reveal that some of the organoclay layers are finely and homogeneously dispersed in the PCL matrix, indicating the formation of nanocomposites having semi-exfoliated structures beside the semi-intercalated structures [44], [6], and suggesting moderate interactions between the organoclay nanoparticles and the polymeric chains [69], [70] in the sequence: Cloisites 20A < Cloisites 15A. In contrast, when the organoclay content is 10 wt%, the homogeneous dispersion of nanoparticles in PCL matrix is difficult and the silicate layers′ stacks are less and less able to exfoliate because they have a strong tendency to interact together to form nanoparticle agglomerates rather than to disperse homogeneously in PCL matrix [55] [Figs. 25 (b) and 26 (b)].

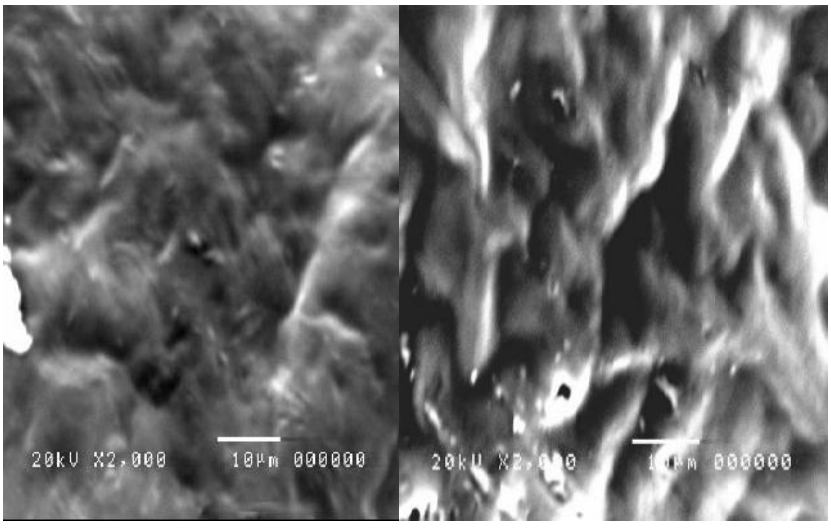

(a) (b)

Fig. 24 SEM micrographs: PCL-5 wt% of Cloisite Na^+ (a) and PCL-10 wt% of Cloisite Na^+ (b)

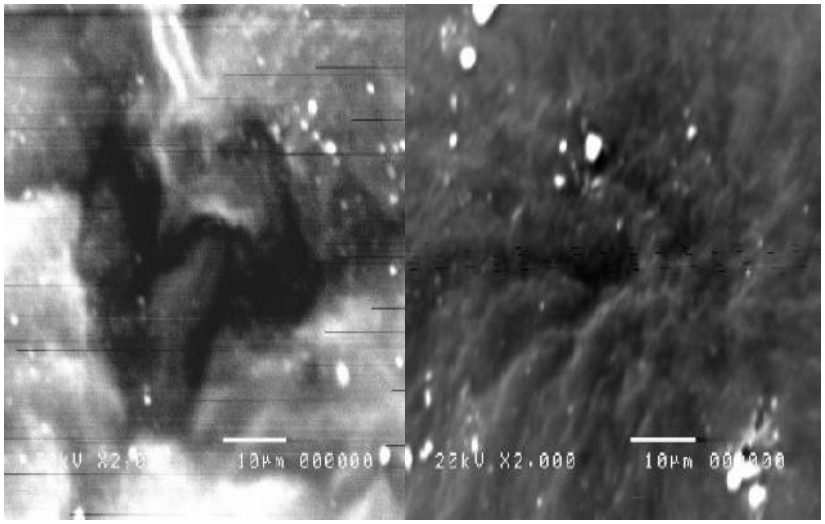

(a) (b)

Fig. 25 SEM micrographs: PCL-5 wt% of Cloisite 20A (a) and PCL-10 wt% of Cloisite 20A (b)

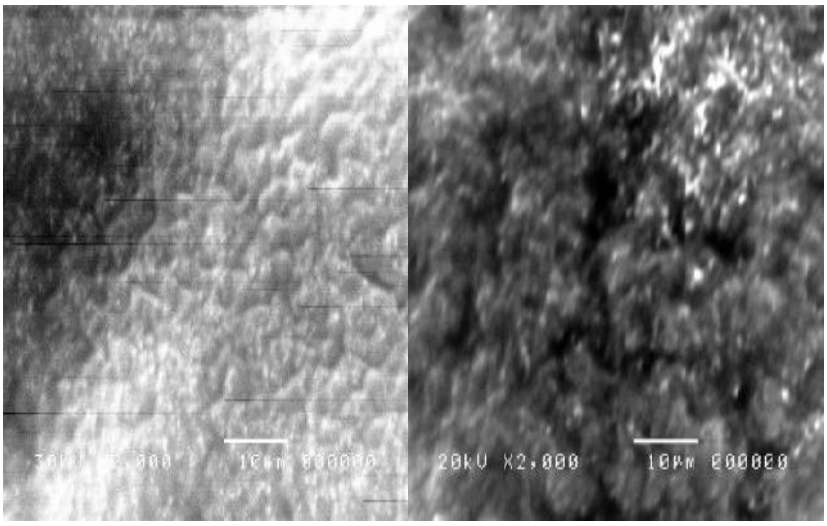

(a) (b)

Fig. 26 SEM micrographs: PCL-5 wt% of Cloisite 15A (a) and PCL-10 wt% of Cloisite 15A (b)

In conclusion, the interaction between the PCL and the clay particles is an important factor in the morphological development of PCL/clay composites.

IV. Conclusions

The thermal stabilities, electrical conductivities, and activation energies of PCL/Cloisite Na^+, Cloisite 20A, and Cloisite 15A composites have been investigated, with the aim to study the influence of organic modifier loading on the dispersibility of the three clays in PCL matrix. The obtained results lead to the following conclusions:

- The organic modifier of Cloisites 20A and 15A lowers the surface energy of the silicate layers and enhances the miscibility between the silicate layers and the polymer matrix.
- Thermal analysis of the obtained composites shows that in the presence of nitrogen flow the incorporation of 5 and 10 wt% of filler brings some decrease in PCL thermal stability in the sequence: Cloisite Na+>Cloisite 15A > Cloisite 20A, while in the presence of air flow these fillers scarcely influence the thermoxidative stability of PCL by slightly accelerating the process.
- The electrical conductivity of PCL is enhanced by introducing Cloisite Na+, Cloisite 20A, and Cloisite 15A at 5 wt% in the sequence: Cloisite Na+> Cloisite 20A> Cloisite 15A. The temperature dependence of the conductivity shows that the prepared composites are semiconductor-like.
- The activation energy (E_σ) is determined by measuring electrical conductivities and it is the lowest for the nanocomposite containing 5 wt% of Cloisite 15A,

showing that it is easily excited and can be employed for electronic and microwave nanodevices as a semiconductor.

- FTIR spectroscopy confirms the van der Waals interaction forces between the clay surface alkyl groups and the PCL chains.
- Studies of XRD and SEM analyses reveal partial intercalated structures in PCL/NaMMT composites and semi-intercalated/semi-exfoliated structures in PCL/ OMMT nanocomposites containing 5 wt% of Cloisite 20A or Cloisite 15A.

REFERENCES

[1] R. Rothon, Particulate-Filled Polymer Composites, 1st ed. Longman Scientific: Harlow UK, 1995.
[2] S. J. Ahmadi; Y.D. Huang; W. Li, J Mater Sci 2004, 39, 1919-1925.
[3] Y. Fukushima; S. J. Inagaki, Inclusion Phenomena 1987, 5, 473.
[4] A. Okada; M. Kawasumi; T. Kurauchi; O. Kamigaito, Polym. Preparation 1987, 28, 447.
[5] Z. Sedlakova; J. Plestil; J. Baldrian,; M. Slouf,; P. Halub, Polym Bull 2009, 63; 365- 384.
[6] I. Turku and T. Karki, Journal of Thermoplastic Composite Materials 2014, 27(2) 180–204.
[7] T. J. Pinnavaia; G.W. Beal, Polymer-Clay Nanocomposites; Wiley, 2000.
[8] Y. Xi; Z. Ding; H. He; R.L. Frost, Colloid Interface Sci 2004, 277, 116-120.
[9] Y. Hu; L. Song; J. Xu; L.Yang; Z. Chen; W. Fan, Colloid Polym Sci 2001, 279, 819-822.
[10] R. K. Bharadwaj, Macromolecules 2001, 34, 9189.
[11] G. Beyer, Fire Mater 2001, 25, 193.
[12] L. Berlund, Fillers and Additives for Plastics 2000, 4,31.
[13] A. Leykin; M. Loelovich; O. Figovsky, Polymer composites Eurofillers 2003 International Conference, Alicante (SPAIN) September 2003, 8-11, P363-364.
[14] J.W. CHo; D.R. Paul, Polymer 2001, 42, 1083.
[15] I. J. Chin; T.T. Albrecht; H.C. Kim; T.P. Russell; J. Wang, Polymer 2001, 42, 5947.
[16] S. Wang; C. Long; X. Wang; Q. Li; Z. Qi, J Appl Polym Sci 1998, 69, 1557.
[17] E. Manias; A. Touny; L. Wu; K. Strawhecker; B. Lu; T.C. Chung, Chem Mater 2001, 13, 3516.
[18] C. Zhao; H. Qin; F.Gong; M. Feng, S. Zhang; M. Yang, Polym Degrad Stab 2005, 87, 183-189.
[19] E. P. Glanellis, Adv Mater 1996, 8, 29-35.
[20] G. Jimenes; N. Ogata; H. Kawai; T. Ogihara, J Appl Polym Sci 1997, 64, 2211.
[21] H. L. Tyan; C. M. Leu; K. H. Wei, Chem Mater 2001, 13, 222.
[22] Y. I. Tien.; K. H. Wei, Polymer 2001, 42, 3213.
[23] T. Peprnicek; J. Duchet; L. Kovarova; J. Malac; J. F. Gerard; J. Simonik, Polym Degrad Stab 2006, 91, 1855.
[24] X. Fu; S. Qutubuddin, Polymer 2001, 42, 807-813.
[25] Y. Li; B. Zhao; S. Xie; S. Zhang, Polym Int 2003, 52, 892.
[26] P. Uthirakumar; K.S. Nahm; Y. B. Hahn; Y.S. Lee, European Polymer J 2004, 40, 2437-2444.
[27] C. Zeng; L. Lee, J. Macromolecules 2001, 34, 4098.
[28] I Engelberg and J. Kohn, Biomaterials 1992,12,292.
[29] H. Tsuji, T. Ishizaka, Macromolecular Bioscience 2001, 1 (2), 59-65.
[30] C. De Kesel; C. Vander Wauven; C. David, Poly Degrad Stab 1997, 55 (1), 107-113.
[31] U. S Ishiaku; K.W. Pang; W. S. Lee; Z. A. Mohd Ishak, European Polymer 2002, 38 (2), 393-401.
[32] R.W. Rees, Encyclopedia Polym Sci Eng, 1985, p. 395. J.E. Mark John Wiley and Sons NY.
[33] R.P. Singha; J.K. Pandey; D. Rutot; P. Degée; P. Dubois, Carbohyd Res 2003,338, 1759–1769.
[34] Q.H. Zeng; A.B. Yu; G.Q. Lu; D.R. Paul, J Nanosci Nanotechnol 2005, (5) 1574–1592.
[35] B. Lepoittevin; M. Devalckenaere; N. Pantoustier; M. Alexandre; D. Kubies; C. Calberg, Polymer 2002,43, 4017–4023.
[36] Y. Di; S. Iannace; E.D. Maio; L. Nicolais, J Polym Sci Part B Polym Phys 2003,41, 670–678.
[37] M.A. Paul; M. Alexandre; P. Degee; C. Henrist; A. Rulmont; P. Dubois, Polymer 2003, 44, 443–450.
[38] R. C. Mackenzie, The Differential Thermal Investigation of Clays; Mineralogy Society: London, 1957.
[39] L. M. Stadtmueller; K. R Ratinac; S. P. Ringer, Polymer 2005, 46, 9574-9584.
[40] J. Zheng; R. Ozisik; R.W. Siegel, Polymer 2006, 47, 7792, 7793.
[41] G. Sivalingam; G. Madras, Polym Degrad Stab 2004, 84 (3), 393-398.
[42] A. C. Draye; O. Persenaire; J. Brožek; J. Roda; T. Košek; Dubois, Polymer (2001), 42 (20), 8325-8332.
[43] O. Persenaire; M. Alexandre; P. Degée; P. Dubois, Biomacromolecules 2001, 2 (1), 288-294.
[44] S. I. Marras; K. P. Kladi; I. Tsivintzelis; I. Zuburtikudis; C. Panayiotou, Acta Biomaterialia 2008, 4, 756–765.
[45] S. I. Marras; I. Zuburtikudis; C. Panayiotou, European Polymer J 2007,43, 2191-2206.
[46] F. Bellucci; G. Camino; A. Frache; A. Sarra, Polym Degrad Stab polymer 2007, 92 (3), 425-436.
[47] J.W. Gilman; C. L. Jackson; A. B. Morgan; R. Harris; E. Manias; E.P. Giannelis, Chem Mater 2000, 12,1866.
[48] M. Zanetti; G. Camino; P. Reichert; R. Mulhaupt, Macromol Rapid Commun 2001, 22,176.
[49] K. Fukushima; D. Tabuani; G. Camino, Materials Science and Engineering C 2009, 29 (4), 1433-1441.
[50] H. Essawy; A. Badran; A. Youssef; A. Abd El-Hakim, Polym Bull 2004,53, 9-17.
[51] Y. Tain; H. Yu; S.S Wu; G.D. Ji, J Mater Sci Lett 2004, 39, 4301.
[52] Y. Cai; Y. Hu; L. Song; L. Lui; Z.Wang; Z. Chen,; W. Fan, J Mater Sci 2007, 42, 5785-5790.
[53] H. Azizi; J. Morshedian; M. Barikani; M. H. Wagner, Express Polym Lett 2010, 4, 252.
[54] X. Zhang; R. Xu; Z. Wu, Polym Int 2003, 52, 790.
[55] T. K. Chen.; Y.I. Tein; K.H. Wei, Polymer 2000, 41, 1345-1353.
[56] Y. S. Choi; M.H. Choi; K. H. Wang; S.O Kim; Y. K. Kim.; I. J. Chung, Macromolecules 2001, 34, 8978-8985.
[57] I. Tien.; K. H. Wei, Macromolecules 2001, 34, 9048.
[58] A. Pattanayak; S.C. Jana, Polymer 2005, 46, 3275-3288.
[59] A. Cheng; S. Wu; D. Jiang; F. Wu; J. Shen, Colloid Polym Sci 2006, 284, 1057-1061.
[60] E. P. Goodings, Chem Soc Revs 1976, 5, 95-119.
[61] G. Kemeny; S. D. Mahanti, Proc Natl Acad Sci USA 1975, 72, 999.
[62] A. E. Pochetennyi; E.V. Ratnikov, Dokl Akad Nauk Bssr 1981, 25, 896.
[63] E. Marton; C. Marton, Methods of Experimental Physics 16-Part B, Chpt. 6,7, 1980.
[64] S.T Oh.; C.S, Ha.; W. J, Cho. J Appl Polym Sci 1994, 54, 859.
[65] J. A. Grapski; S. L. Copper, Biomaterials 2001, 22, 2239.
[66] L. Song.; Y Hu.; Y. Tang.; R. Zhang; Z. Chen.; W. Fan, Polym Degrad Stab. 2005,87, 111.
[67] D.i. Yingwei; S. Iannace; E. D. Maio; L. Nicolais, Journal of Polymer Science Part B: Polymer Physics 2003, 41, 670–678.
[68] J. Zhu; P. Start; K. A. Mouritz; C. A. Wilkie, Polym Degrad Stab 2002, 77, 253-258.
[69] M. Zanetti; G. Camino; R. Thomann; R. Mulhaupt, Polymer 2001, 42, 4501- 4507.
[70] X. L. Xie; R.K.Y Li; Q. X Liu; Y.W. Mai, Polymer 2004, 45, 2796.